# Profiles of Intraocular Pressure in Human Donor Eyes during Femtosecond Laser Procedures—A Comparative Study

*Clemens Strohmaier, Christian Runge, Orang Seyeddain, Martin Emesz, Christian Nischler, Alois Dexl, Günther Grabner, and Herbert A. Reitsamer*

**Purpose.** To compare four different femtosecond laser devices (IntraLase FS, Zeiss VisuMAX, and Ziemer Femto LDV, and a prototype Schwind SmartTech Nanolaser) in human donor eyes with regard to their effects on IOP during femtosecond laser flap cutting. In order to get cuts parallel to the corneal surface, the cornea has to be forced into a defined shape and current femtosecond laser devices either use a flat or a curved patient interface design to achieve applanation.

**Methods.** IOP was measured in enucleated eyeballs ($n = 46$) not suitable for keratoplasty by direct cannulation of the vitreous body. A second cannula was inserted to adjust IOP to a baseline pressure of 20 mm Hg. The eyeballs were lifted by custom made supporting stands to achieve an appropriate height and put under the femto-LASIK devices.

**Results.** The flat patient interfaces gave rise to higher IOPs (IOP max = 328.3 ± 29.8, 228.8 ± 28.4, and 201.09 ± 21.4 mm Hg), whereas the curved patient interface caused lower IOPs in response to attachment and suction (IOP max = 104.9 ± 13.4 mm Hg).

**Conclusions.** Based on previous findings of visual field defects after LASIK, and as a consequence of the present study, it seems feasible to design patient interfaces in a more physiologic manner to prevent high IOPs during refractive procedures. (*Invest Ophthalmol Vis Sci.* 2013;54:522–528) DOI:10.1167/iovs.12-11155

LASIK has, over the last years, become by far the most frequent corneal refractive surgery procedure for the correction of all types of ametropias performed worldwide today. During surgery, creation of the corneal flap with the mechanical microkeratome still remains the technical step associated with the highest risk of significant complications, such as a button hole, incomplete, or lost caps and flaps being thinner in the center than in the periphery ("meniscus"-like shaped),[1–3] as well as long term complications, such as epithelial ingrowth or corneal ectasia.[4,5]

Therefore, the newer technique using a femtosecond laser has rapidly been embraced by refractive surgeons over the last years with 47% of the LASIK procedures in the United States being the performed with the IntraLase (Abbott Medical Optics Inc., Irvine, CA) in 2007. Although this has led to the emergence of previously unknown complications, (e.g., transient light sensitivity syndrome [TLSS]), in the early models with only lower repetition rates available, the fast development of lasers with higher frequency and lower pulse energy has all but eliminated this finding.[6] In general, it is felt that the newer generations of femtosecond lasers, and the emerging competition in the field with several companies developing advanced and more sophisticated machines (e.g., 20/10 Perfect Vision; Femtec, Heidelberg, Germany; Femto LDV Laser; Ziemer Ophthalmic Systems, Port, Switzerland; and VisuMax; Carl Zeiss Meditec, Jena, Germany) has increased safety significantly, as recently reported in a large series of sub-Bowman's keratomileusis with a low intra- and postoperative complication rate of only 0.63%,[7] which, besides obvious patient safety, is also important for cost coverage by insurances, as discussed in several countries.[8]

During the creation of the superficial flap an increased IOP[1] is induced by basically all types of suction rings used to both stabilize the cornea and increase ocular rigidity for precise cutting, be it either mechanical or with the femtosecond laser technology.

Again, several complications have been reported to occur due to this IOP rise, such as optic neuropathy[9,10] visual field loss,[11] and cilioretinal artery occlusion.[12] Using scanning laser polarimetry[13] and optical coherence tomography[14–16] retinal nerve fiber layer thickness has been evaluated following LASIK with still ambiguous results.

Other complications possibly related to abrupt changes in IOP during the flap cut include retinal breaks and retinal detachment, premacular hemorrhage, and central retinal artery occlusion.[14–16] To the best of our knowledge, no increase in any of these complications has been reported in case series using a femtosecond laser system as compared with a mechanical microkeratome yet.

Several experimental papers have been published in the peer reviewed literature studying IOP changes during mechanical or femtosecond-assisted flap creation either in animal or human donor eyes. An overview of the scientific literature is given in Table 1.

It is the aim of this experimental study to measure pressure profiles in vitro during a complete femtosecond laser flap cutting procedure resembling a clinical set up in human donor eyes as closely as possible and to compare four femtosecond

From the Department of Ophthalmology, University Hospital Salzburg/Paracelsus Medical University, Salzburg, Austria.

Supported by grants from the Austrian Academy of Sciences (DOC 22926 [CS]), the Paracelsus Medical University (FFF R09/01/001-REI), the Fuchs Foundation for Research in Ophthalmology (G27), the Adele-Rabensteiner Foundation of the Austrian Ophthalmological Society, and an institutional grant from the University Eye Clinic Salzburg.

Submitted for publication October 16, 2012; revised December 4, 2012; accepted December 6, 2012.

Disclosure: **C. Strohmaier**, None; **C. Runge**, None; **O. Seyeddain**, None; **M. Emesz**, None; **C. Nischler**, None; **A. Dexl**, None; **G. Grabner**, None; **H.A. Reitsamer**, None

Corresponding author: Herbert A. Reitsamer, University Eye Clinic, Paracelsus, Medical University Salzburg, Universitätsklinikum, St.Johanns-Spital, Müllner Hauptstrasse 48, A 5020 Salzburg, Austria; h.reitsamer@salk.at.



Investigative Ophthalmology & Visual Science, January 2013, Vol. 54, No. 1

**Table 1.** Overview of the Currently Available Reports of Maximum IOP during Corneal Flap Cutting with Either a Femto Second Laser or a Microkeratome

| | | |
|---|---|---|
| Femtolaser | | |
| Intralase/flat PI | Porcine/enucleated | 119.33 ± 15.88 mm Hg[27] |
| Visumax/curved PI | Rabbit/in vivo | 81.78 ± 6.55 mm Hg[20] |
| Intralase/flat PI | Porcine/enucleated | 260 ± 53 mm Hg[28] |
| Intralase/flat PI | Porcine/enucleated | 135 ± 16 mm Hg[29] |
| Visumax/curved PI | Porcine/enucleated | 65 ± 20 mm Hg[29] |
| Femtec/flat PI | Porcine/enucleated | 205 ± 32 mm Hg[29] |
| Femto LDV/flat PI | Porcine/enucleated | 184 ± 28 mm Hg[29] |
| Visumax/curved PI | Rabbit/in vivo | 26.8 ± 1.2 mm Hg[19] |
| Intralase/flat PI | Human/enucleated | 328.3 ± 29.8 mm Hg* |
| Intralase/flat PI | Human/enucleated | 192.6 ± 27.7 mm Hg* |
| Visumax/curved PI | Human/enucleated | 88.9 ± 8.2 mm Hg* |
| Microkeratome | | |
| Amadeus | Porcine/enucleated | 318 ± 59 mm Hg[28] |
| Moria M2 | Rabbit/in vivo | 141.02 ± 20.46 mm Hg[20] |
| Moria M2 | Porcine/enucleated | 160.52 ± 22.73 mm Hg[27] |
| Moria | Porcine/enucleated | 113.65 ± 10.78 mm Hg[30] |
| Moria | Human/enucleated | 175.8 ± 37.6 mm Hg[31] |
| Innovatome | Human/enucleated | 151.8 ± 27.4 mm Hg[31] |
| Hansatome | Human/enucleated | 154.7 ± 33.8 mm Hg[31] |
| BD K-3000 | Porcine/enucleated | 99.1 ± 6.1 mm Hg[32] |
| Universal Keratome | Human/enucleated | 108.0 ± 22.1 mm Hg[33] |
| Keratek | Porcine/enucleated | 360 ± 35 mm Hg[34] |
| Corneal shaper | Porcine/enucleated | 140 ± 22 mm Hg[34] |

The table shows the instrument, the patient interface (PI) and the experimental model that were used, as well as the maximum IOP that was reached during the procedure. All microkeratomes have flat designed PIs. Details on the experimental conditions can be reviewed in the references given on the right side of the table.

* Strohmaier C, et al. IOVS 2008;49: ARVO E-Abstract 2914.

laser systems, IntraLase FS, Zeiss VisuMAX, Ziemer Femto LDV, and a prototype of the Schwind SmartTech Laser (Schwind, Kleinostheim, Germany), with identical experimental settings.

## Methods

All experiments were reviewed and approved by the ethics committee of the state of Salzburg and conducted in compliance with the Declaration of Helsinki..

Human donor eyes not suited for corneal transplantation were obtained from the local eye bank ($n = 46$, average age of donors 63.5 ± 12.3 years). For the femto-LASIK procedures the eye balls were placed on a supporting stand manufactured for this purpose. The vitreous compartment was cannulated with a 27 gauge needle and connected to a water column in order to adjust the baseline IOP before starting the measurements. For measurements of IOP, a second cannula was inserted into the vitreous compartment. The cannula was connected to a pressure transducer of an electronic data acquisition system (PowerLab; ADInstruments, Grand Junction, Colorado). Small amounts of superglue around the insertion site were used to keep the seal water tight. The measurement protocol followed the standard surgical LASIK protocols of the four femto laser instruments subjected to the present investigation (IntraLase FS, Zeiss VisuMAX, Ziemer Femto LDV, and Schwind SmartTech Laser). Figure 1 shows OCT images of the two types of patient interfaces used (flat versus curved).

### Intralase FS Protocol

After the eye ball was cannulated, as described above, the patient interface was placed on the cornea and suction was applied with the syringe-locking thumb activator in a typical way. The setup was then moved under the laser and the surgeon lowered the laser. Before the laser was locked into the patient interface, the stop cock to the water column was closed to prevent water draining from the eye ball in case IOP would rise during the experiment. The laser was then lowered toward the eye and the pressure on the eye ball was increased until a green light indicated that the device was ready to engage the laser (low green condition). The laser was triggered by the surgeon and after the cutting procedure was over, the laser and the patient interface were removed from the eye. In a second series of experiments the laser was lowered until a red light indicated that the pressure exerted on the eye ball was too high. The device was then withdrawn until the red light changed to green and the laser was engaged ("high green" condition). An example of this protocol is shown in Figure 2.

### Zeiss Visumax Protocol

After the eye ball was instrumented as described above, the patient interface was mounted on the laser and the suction tubing was connected to the built in vacuum port on the VisuMax. Before the patient interface touched the eye, the stop cock to the water column was closed to prevent water from leaving the eye ball in case IOP would rise during the experiment. In order to make contact, the patient platform was elevated toward the laser/patient interface. After contact, suction was applied to the interface. When a stable vacuum was achieved, the trigger was cleared and the surgeon engaged the laser cutting procedure. After having finished the cut, the vacuum to the interface was released and the interface was removed from the eye. An example of this protocol is shown in Figure 3.

### Ziemer Femto LDV Protocol

After the eye ball was instrumented as described above, the hand held laser delivery system with the patient interface was advanced toward

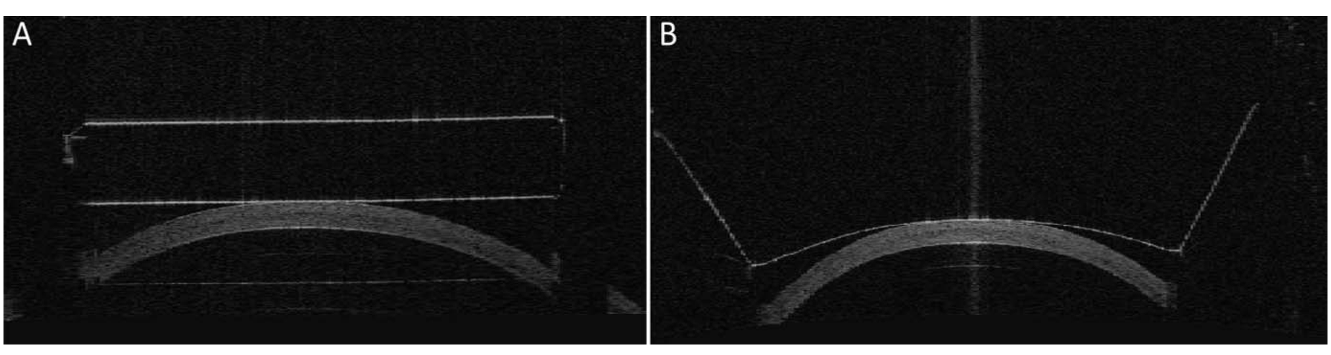


**Figure 1.** Differently shaped patient interfaces imaged with the Zeiss Visante OCT. (**A**) Flat patient interface design as used by IntraLase FS, Ziemer Femto LDV, and the experimental interface of the Schwind SmartTech Laser. (**B**) Curved interface design as used by the Zeiss VisuMax femtolaser. The displaced volumes of the two shapes are 250 μL for the flat design and 120 μL for the curved design during applanation.

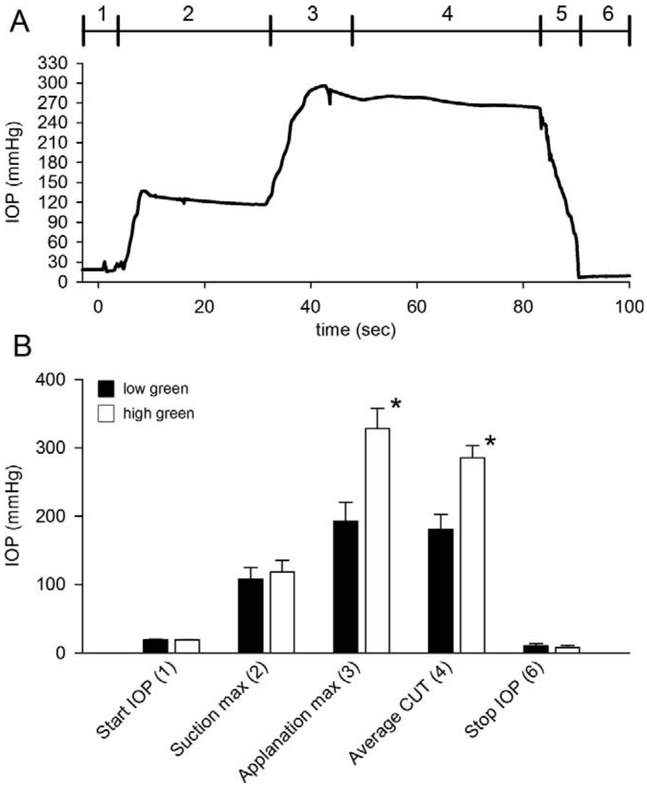


**FIGURE 2.** IntraLase FS femto procedure. (**A**) Single tracing of IOP during a femto LASIK procedure. Starting IOP after closure of the stop cock to the water column (*1*), positioning of the patient interface and application of suction vacuum (*2*), lowering of the laser onto the patient interface and forcing the interface against the eye, the down force was adjusted to meet the cutting criteria (*green light*) (*3*), cutting period (*4*), withdrawal of the laser with release of suction vacuum (*5*), spontaneous IOP after procedure with closed stop cock (*6*). (**B**) Average IOP values during the selected periods mentioned above. *Black bars* represent the pressures measured during "low green" conditions ($n = 8$), *white bars* represent pressures during "high green" conditions ($n = 7$) (for details see Methods section). *Asterisk* indicates $P \leq 0.05$.

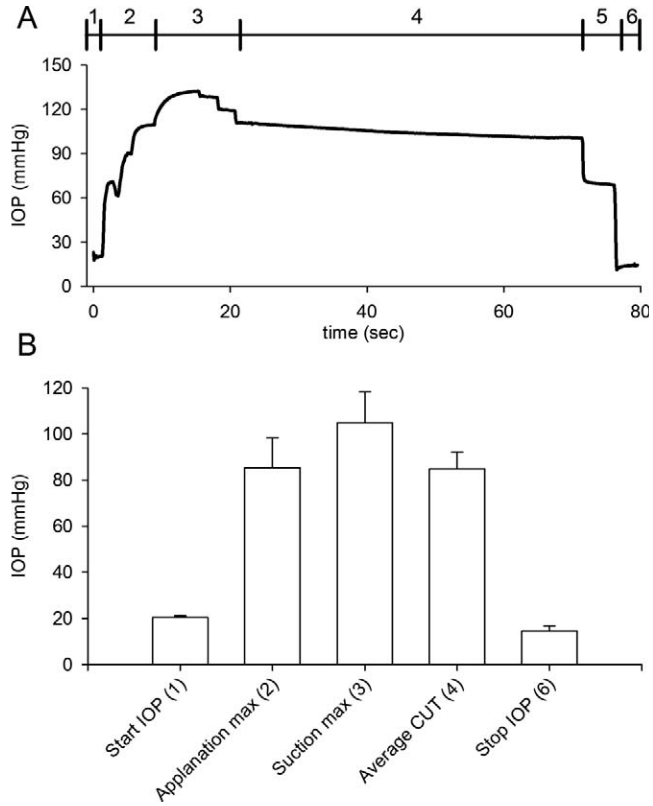


**FIGURE 3.** Zeiss VisuMax femto procedure. (**A**) Single tracing of IOP during a femto LASIK procedure. Starting IOP after closure of the stop cock to the water column (*1*), lowering of the laser onto the patient interface and forcing the interface against the eye (*2*), application of suction vacuum, the down force was automatically adjusted by the device (*3*), cutting period (*4*), withdrawal of the laser with release of suction vacuum (*5*), spontaneous IOP after the procedure with closed stop cock (*6*). (**B**) Average IOP values during the selected periods mentioned above ($n = 11$).

and placed onto the cornea. Before the patient interface touched the eye, the stop cock to the water column was closed to prevent water from leaving the eye ball in case IOP would rise during the experiment. After contact, suction was applied to the interface. When a stable vacuum was achieved the trigger was cleared and the surgeon started the laser cutting procedure. After having finished the cut, the vacuum to the patient interface was released, the laser delivery system dislodged and the interface removed from the eye. An example of this protocol is shown in Figure 4.

### Schwind Smarttech Laser

After the eye ball was instrumented as described above, the experimental flat design patient interface was mounted on the laser and the suction tubing was connected to the built in vacuum port of the Schwind SmartTech Laser. Before the patient interface touched the eye, the stop cock to the water column was closed to prevent water from leaving the eye ball in case IOP would rise during the experiment. In order to make contact, the patient interface was lowered onto the eye. After contact, suction was applied to the interface. When a stable vacuum was achieved, the trigger was cleared and the surgeon started the laser cutting procedure. After having finished the cut, the vacuum to the patient interface was released and the interface was removed from the eye. An example of this protocol is shown in Figure 5.

All data are shown as the mean ± 95% confidence intervals. For statistical analysis of effects two way repeated measurements ANOVA was used. Differences between groups were calculated using a post hoc strategy with Bonferroni adjustments.

## RESULTS

Table 2 shows the mean IOP values measured in the different phases of the femto laser cutting procedure for all four devices. A corresponding, representative tracing for each single device is given in the Figures 2 to 5, respectively.

## DISCUSSION

### Why Is It Important to Know IOPs during LASIK Procedures?

As mentioned in the introduction, several pathologies of the retina and the optic nerve head were reported in relation to the creation of corneal flaps using patient interfaces with suction rings and flat designs, both with mechanical microkeratomes as well as femtosecond laser devices. However, it is not clear, if IOP alone is the reason for the observed pathologies after LASIK. Distortion and shear stress of the eye ball as caused by the suction interface with resulting changes in the biomechanics also seem possible explanations

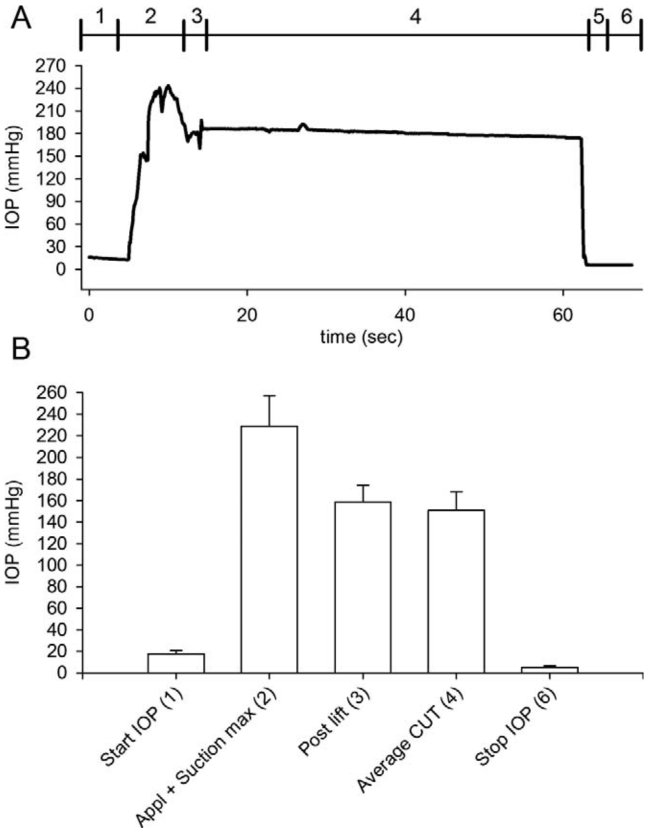


**FIGURE 4.** Ziemer Femto LDV procedure. (**A**) Single tracing of IOP during a femto LASIK procedure. Starting IOP after closure of the stop cock to the water column (*1*), lowering of the hand held laser delivery system with the patient interface onto the eye, forcing the interface against the eye (*2*), application of suction vacuum (*3*), cutting period (*4*), withdrawal of the laser with release of suction vacuum (*5*), spontaneous IOP after procedure with closed stop cock (*6*). (**B**) Average IOP values during the selected periods mentioned above ($n = 11$).

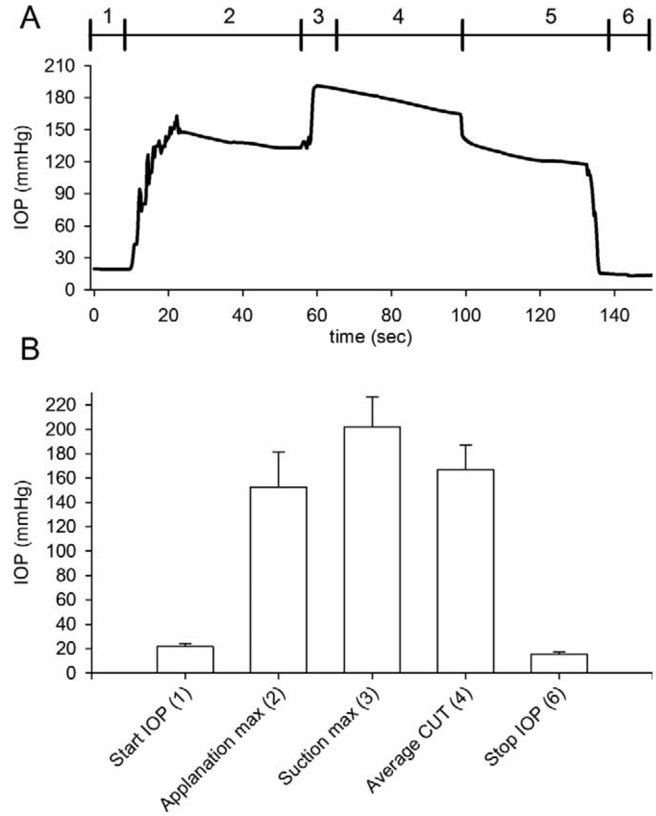


**FIGURE 5.** Schwind SmartTech procedure with experimental flat patient interface. (**A**) Single tracing of IOP during a femto LASIK procedure. Starting IOP after closure of the stop cock to the water column (*1*), lowering of the patient interface onto the eye and forcing the interface against the eye (*2*), application of suction vacuum, the down force was automatically adjusted by the device (*3*), cutting period (*4*), withdrawal of the laser with release of suction vacuum (*5*), spontaneous IOP after procedure with closed stop cock (*6*). (**B**) Average IOP values during the selected periods mentioned above ($n = 6$).

for retinal tears and destruction of nerve fibers in the lamina cribrosa. In addition, patients eventually report the experience of fading light and vision turning dark in the treated eye during LASIK and femtosecond laser surgeries, a sensation that is experienced after the application of suction and pressure to the patient interface (personal observations). This could be a result of IOP increased beyond perfusion pressure. As a result, ocular blood flow might be reduced below a critical level,[17,18] or possibly direct transient stress to the optic nerve fibers in the lamina cribrosa might cause the sensations reported by the patients.

As a consequence of the published side effects reportedly linked to LASIK surgery, it was the goal of the present investigation to measure IOP during corneal flap creation using different femto laser systems. The study was performed in human donor eyeballs from the local cornea bank, not suited for corneal transplantation.

## Comparison of the Results of the Study

All femto laser procedures caused a significant increase of IOP at every stage of the cutting sequence and the results of this study make it obvious that the curved patient interface (Zeiss Visumax) elevates IOP less than the flat shaped patient interfaces of the other lasers do. At the "high green" force, the IntraLase FS laser delivered the highest IOP values (328.3 ± 29.8 mm Hg) of all setups tested in the present study.

These findings are similar to the literature as it is summarized in Table 1. Although IOP values vary, due to differences in species (ocular rigidity coefficients), displaced volume within the eye, interface sizes used and also IOP measurement methods, a common finding is a smaller increase in IOP when using curved interface designs and a higher increase in IOP when using flat interfaces.

In addition, and for comparability reasons, it needs to be pointed out that in the publications shown in Table 1, the baseline IOPs were different across the studies. Besides species differences this is important, because the ocular pressure–volume relationship as described by the Friedenwald equation (Equation 1) follows an exponential course. As opposed to a linear relationship, the increase in IOP depends not only on the increase in volume, but also on the starting pressure at baseline. As an example, the papers by Ang and Chaurasia used the same type of patient interface and species (rabbits), but different starting pressures and subsequently reported different pressures.[19,20] In their study, Ang et al.[19] started at a baseline IOP of 9 mm Hg, which increased to 28 mm Hg during femto LASIK flap creation, whereas Chaurasia et al.[20] started at a baseline IOP of 16 mm Hg and reported peak IOPs of 60 mm Hg. While differences in anesthetic protocols might account for the different starting IOPs in these studies, the reported values for IOP in conscious and anesthetized rabbits are 20 to 25 mm Hg and 16 mm Hg, respectively,[21,22] so the higher

TABLE 2. IOPs during Four Comparable Periods of the Experiment

| | IOP (Start) | IOP (Max) | Average IOP (Cut) | IOP (Stop) | *n* |
|---|---|---|---|---|---|
| IntraLase FS; (low green) | 19.3 ± 1.3 | 192.6 ± 27.7 | 180.6 ± 21.6 | 10.12 ± 3.8 | 8 |
| IntraLase FS; (high green) | 19.3 ± 0.6 | 328.3 ± 29.8 | 285.6 ± 17.2 | 7.87 ± 3.2 | 7 |
| Zeiss VisuMax | 20.5 ± 0.6 | 104.9 ± 13.4 | 84.9 ± 7.3 | 14.6 ± 2.2 | 11 |
| Ziemer Femto LDV | 17.7 ± 2.9 | 228.8 ± 28.4 | 150.9 ± 17.2 | 5.08 ± 1.5 | 14 |
| Schwind SmartTech | 20.65 ± 1.9 | 201.09 ± 21.4 | 166.80 ± 17.2 | 14.22 ± 1.5 | 6 |
| *P* value | n.s. | <0.001 | <0.001 | n.s. | |

The differences between the four protocols are highly significant at the maximum IOP during the procedure and the average IOP during the cutting procedure. There is no significant difference between the protocols at IOP Start and at IOP Stop. All data are shown as mean ± 95% confidence interval.

pressures reported by Chaurasia et al.[20] reflect IOP raises under physiologic conditions more closely.

As a consequence, in the present study, the baseline IOPs in all groups was kept within a narrow range to eliminate the bias that would be introduced otherwise. No significant difference in baseline IOPs was found between groups (Table 2).

## How Do Human Donor Eyes Compare with Living Human Eyes?

When choosing a model to investigate the situation in living humans, it is important to consider the shortcomings of the model. In terms of its relevance to its pressure–volume relationship the main difference between dead and living eyes is the lack of blood flow and blood pressure on the arterial as well as on the venous side of the circulation. This is supported by previous investigations clearly showing marked differences in ocular rigidity between eyes before and after enucleation.[23,24] Figure 6 shows the course of IOP in a rabbit eye in response to continuous infusion of balanced salt solution into the vitreous cavity as shown by Kiel before.[25] The graph clearly demonstrated the marked difference between the IOP course predicted by the Friedenwald equation (Equation 1) and the IOP course in a living eye where IOP increases in a polyphasic manner.

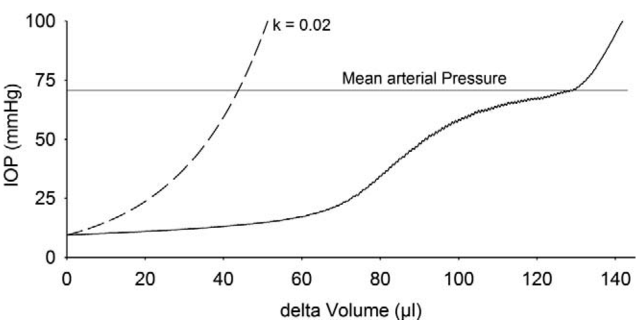


FIGURE 6. Pressure–volume (P/V) relationship in a rabbit eye. The long dashed line shows the P/V relationship as calculated by the Friedenwald equation in post mortem eyes using an ocular rigidity coefficient of k = 0.02. The solid line shows the P/V relationship in a living rabbit eye. Two fundamental differences can be observed between the curves. The Friedenwald equation describes an exponential increase in IOP for additional aliquots of volume added to the eye, however, the real world IOP response to a continuous infusion of fluid results in a polyphasic behavior of IOP (*solid line*, infusion rate 120 µL/min). The differences are primarily caused by the fact that in living eyes, the intraocular vasculature is filled with blood, pressed into the eye by the local arterial and venous blood pressure. Increasing IOP acts against the blood pressure and the volume of the vasculature will be expelled from the eye accordingly (*solid line*). Once the vasculature is empty (at IOP > MAP), the PV relationship follows an exponential function. Since in human donor eyes the intraocular vasculature is not filled with blood, no fluid can be expelled by increasing IOP and consequently the pressure volume relationship follows an exponential function as predicted by the Friedenwald equation (*dashed line*).

$$IOP_2 = 10^{(KdV + \log IOP_1)} \qquad (1)$$

The Friedenwald equation describes the pressure–volume relationship in relation to the rigidity of the eye (rigidity factor k). The higher the rigidity of the eye, the higher the increase in IOP in response to a certain increase in intraocular volume.

Based on the assumption that the pressure volume relationship in the living and the dead eye is different, and that the same volume added to a dead eye causes a much higher increase in IOP than in the living eye, one can use the pressure volume relationship from the literature[26] and try to estimate IOP during applanation with a patient interface. The difference between the corneal shape and the shape of the patient interface defines a volume, which can be estimated as the intraocular volume change that causes the rise in IOP. The displaced volume cannot be estimated accurately because the peripheral shape of the patient interface where the cornea, conjunctiva, and sclera are sucked into the device is complex, and the extent to which the anatomical structures follow the complex shape of the interface is only vaguely known. However, a rough approximation with a simplified model gives some insight into the pressures, which might be expected in living human eyes.

The pressure rise using flat interface designs is generally higher than the IOP caused by a curved interface (Table 2). Figure 7 shows a pressure/volume relationship of a human

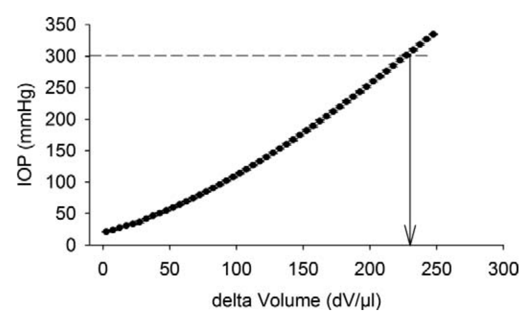


FIGURE 7. Pressure Volume relationship in a human donor eye. The exponential function of a dead human donor eye is well fit by a simple polynomial equation: $IOP = 16.09 + 0.73 \times dV + 0.0024 \times dV^2$ ($R^2 = 1$, $P < 0.05$). Based on these functions and the estimation of intraocular blood volumes it is possible to try to estimate the real pressure in living human eyes during femto laser procedures with flattened corneas by patient interfaces. Depending on the donor eye, an increase of IOP to 250 to 300 mm Hg is caused by adding roughly 200 to 250 µL of physiologic saline solution to the intraocular volume (*arrow*).

donor eye as used for the present investigations. As predicted by the Friedenwald equation, the response of IOP to a continuous infusion of physiologic saline solution follows an exponential function ($IOP = 16.09 + 0.73 \times dV + 0.0024 \times dV^2$ [$R^2 = 1$, $P < 0.05$]); dv indicates volume increment. In order to achieve an increase in IOP of 250 to 300 mm Hg, a fluid volume of roughly 200 to 250 μL has to be infused into the eye. Given the fact that the uveal blood volume is estimated to be approximately 250 μL, the rise in IOP should be limited to the value of mean arterial pressure. From our own observations during femtosecond LASIK procedures we know that most patients describe fading of the light and complete loss of light perception. The varying descriptions might be caused by differences in the ocular rigidity coefficients and probably also the differences in arterial pressures of the individual patients under these stressful surgical conditions. In addition it is unknown if the whole blood volume of the living eye is expelled or if it is only a fraction of the total volume. The question seems reasonable given the fact that the pressure rise occurs much faster when the patient interface is applied as opposed to the slow infusion model we used in the present study.

The IOP values obtained in the present study can, therefore, be regarded as the upper limit of the expected IOP range during the femto LASIK procedure, while the individual mean arterial blood pressure of the patient is the lower limit of the expected pressure range during the cutting procedure. The range of possible IOPs explains the variable sensations of patients in our daily practice.

## Conclusions

Based on the present data it seems safe to conclude that substantial pressure elevations occur during femto-LASIK procedures and these findings are in accordance with the results published by others. Furthermore, the results of the present study clearly demonstrate that curved patient interface designs cause a smaller increase in IOP than flat designs. To the best of the author's knowledge, no systematic longitudinal observations of the nerve fiber layer, visual fields, and the optic disk have been performed. However, considering the present and previous results on IOP elevations by several, widely used patient interfaces, the data clearly provide the rationale for such investigations.

## *References*


1. Arevalo JF, Ramirez E, Suarez E, et al. Rhegmatogenous retinal detachment in myopic eyes after laser in situ keratomileusis. Frequency, characteristics, and mechanism. *J Cataract Refract Surg*. 2001;27:674–680.
2. Ruiz-Moreno JM, Perez-Santonja JJ, Alio JL. Retinal detachment in myopic eyes after laser in situ keratomileusis. *Am J Ophthalmol*. 1999;128:588–594.
3. Rodriguez A, Camacho H. Retinal detachment after refractive surgery for myopia. *Retina*. 1992;12:S46–50.
4. Wenzl E, Ardjomand N. Epithelial ingrowth 12 years after LASIK. *Spektrum Der Augenheilkunde*. 2010;24:237–239.
5. Rabinowitz YS. Ectasia after laser in situ keratomileusis. *Curr Opin Ophthalmol*. 2006;17:421–426.
6. Stonecipher KG, Dishler JG, Ignacio TS, Binder PS. Transient light sensitivity after femtosecond laser flap creation: clinical findings and management. *J Cataract Refract Surg*. 2006;32: 91–94.
7. Charteris DG, Cooling RJ, Lavin MJ, McLeod D. Retinal detachment following excimer laser. *Br J Ophthalmol*. 1997; 81:759–761.
8. Burggraf H. Refractive Surgery - a necessary Medical Treatment? *Spektrum Der Augenheilkunde*. 2010;24:330–332.
9. Vilaplana D, Guinot A, Escoto R. Giant retinal tears after photorefractive keratectomy. *Retina*. 1999;19:342–343.
10. Krueger RR, Seiler T, Gruchman T, Mrochen M, Berlin MS. Stress wave amplitudes during laser surgery of the cornea. *Ophthalmology*. 2001;108:1070–1074.
11. Panozzo G, Parolini B. Relationships between vitreoretinal and refractive surgery. *Ophthalmology*. 2001;108:1663–1668. discussion 1668–1669.
12. Flaxel CJ, Choi YH, Sheety M, Oeinck SC, Lee JY, McDonnell PJ. Proposed mechanism for retinal tears after LASIK: an experimental model. *Ophthalmology*. 2004;111:24–27.
13. Tsai YY, Lin JM. Effect of laser-assisted in situ keratomileusis on the retinal nerve fiber layer. *Retina*. 2000;20:342–345.
14. Iester M, Tizte P, Mermoud A. Retinal nerve fiber layer thickness changes after an acute increase in intraocular pressure. *J Cataract Refract Surg*. 2002;28:2117–2122.
15. Gurses-Ozden R, Pons ME, Barbieri C, et al. Scanning laser polarimetry measurements after laser-assisted in situ keratomileusis. *Am J Ophthalmol*. 2000;129:461–464.
16. Gurses-Ozden R, Liebmann JM, Schuffner D, Buxton DF, Soloway BD, Ritch R. Retinal nerve fiber layer thickness remains unchanged following laser-assisted in situ keratomileusis. *Am J Ophthalmol*. 2001;132:512–516.
17. Conway ML, Wevill M, Benavente-Perez A, Hosking SL. Ocular blood-flow hemodynamics before and after application of a laser in situ keratomileusis ring. *J Cataract Refract Surg*. 2010; 36:268–272.
18. Schicke SH, Krumeich J, Duncker GI, Scheibel S, Thielscher M. Retinal colour duplex scanning during LASIK-ring suction with different keratomes. *Graefes Arch Clin Exp Ophthalmol*. 2008;246:1009–1015.
19. Ang M, Chaurasia SS, Angunawela RI, et al. Femtosecond lenticule extraction (FLEx): clinical results, interface evaluation, and intraocular pressure variation. *Invest Ophthalmol Vis Sci*. 2012;53:1414–1421.
20. Chaurasia SS, Luengo Gimeno F, Tan K, et al. In vivo real-time intraocular pressure variations during LASIK flap creation. *Invest Ophthalmol Vis Sci*. 2010;51:4641–4645.
21. Reitsamer HA, Kiel JW. A rabbit model to study orbital venous pressure, intraocular pressure, and ocular hemodynamics simultaneously. *Invest Ophthalmol Vis Sci*. 2002;43:3728–3734.
22. McLaren J, Brubaker R, FitzSimon J. Continuous measurement of intraocular pressure in rabbits by telemetry. *Invest Ophthalmol Vis Sci*. 1996;37:966–975.
23. Eisenlohr JE, Langham ME, Maumenee AE. Manometric studies of the pressure-volume relationship in living and enucleated eyes of individual human subjects. *Br J Ophthalmol*. 1962;46: 536–548.
24. Ytteborg J. The role of intraocular blood volume in rigidity measurements on human eyes. *Acta Ophthalmol (Copenh)*. 1960;38:410–436.
25. Kiel JW. The effect of arterial pressure on the ocular pressure-volume relationship in the rabbit. *Exp Eye Res*. 1995;60:267–278.
26. Silver DM, Geyer O. Pressure-volume relation for the living human eye. *Curr Eye Res*. 2000;20:115–120.
27. Hernandez-Verdejo JL, Teus MA, Roman JM, Bolivar G. Porcine model to compare real-time intraocular pressure during LASIK with a mechanical microkeratome and femtosecond laser. *Invest Ophthalmol Vis Sci*. 2007;48:68–72.
28. Vetter JM, Schirra A, Garcia-Bardon D, Lorenz K, Weingartner WE, Sekundo W. Comparison of intraocular pressure during corneal flap preparation between a femtosecond laser and a

mechanical microkeratome in porcine eyes. *Cornea*. 2011;30: 1150–1154.

29. Vetter JM, Holzer MP, Teping C, et al. Intraocular pressure during corneal flap preparation: comparison among four femtosecond lasers in porcine eyes. *J Refract Surg*. 2011;27: 427–433.
30. Hernandez-Verdejo JL, de Benito-Llopis L, Teus MA. Comparison of real-time intraocular pressure during laser in situ keratomileusis and epithelial laser in situ keratomileusis in porcine eyes. *J Cataract Refract Surg*. 2010;36:477–482.
31. Bradley JC, McCartney DL, Craenen GA. Continuous intraocular pressure recordings during lamellar microkeratotomy of enucleated human eyes. *J Cataract Refract Surg*. 2007;33: 869–872.
32. Bissen-Miyajima H, Suzuki S, Ohashi Y, Minami K. Experimental observation of intraocular pressure changes during microkeratome suctioning in laser in situ keratomileusis. *J Cataract Refract Surg*. 2005;31:590–594.
33. Kasetsuwan N, Pangilinan RT, Moreira LL, et al. Real time intraocular pressure and lamellar corneal flap thickness in keratomileusis. *Cornea*. 2001;20:41–44.
34. Sachs HG, Lohmann CP, Op de Laak JP. Intraocular pressure in sections with 2 microkeratomes in vitro [in German]. *Ophthalmologe*. 1997;94:707–709.